REMOTE SENSING OF ATMOSPHERE, HYDROSPHERE, AND UNDERLYING SURFACE

Air Composition over the Russian Arctic: 1—Methane

O. Yu. Antokhina[a], P. N. Antokhin[a], V. G. Arshinova[a], M. Yu. Arshinov[b], B. D. Belan[a], *,
S. B. Belan[a], E. V. Guruleva[a], D. K. Davydov[a], G. A. Ivlev[a], A. V. Kozlov[a], K. Law[b],
T. M. Rasskazchikova[a], J.-D. Paris[c], D. E. Savkin[a], D. V. Simonenkov[a],
T. K. Sklyadneva[a], G. N. Tolmachev[a], and A. V. Fofonov[a]

[a] *V.E. Zuev Institute of Atmospheric Optics, Siberian Branch, Russian Academy of Sciences, Tomsk, 634055 Russia*
[b] *Laboratoire Atmosphères, Milieux, Observations Spatiales LATMOS, UMR 8190, Paris, France*
[c] *Laboratoire des Sciences du Climat et de l'Environnement, LSCE/IPSL, CNRS-CEA-UVSQ,
Orme des Merisiers, CEA Saclay, Gif-sur-Yvette, France*
*e-mail: bbd@iao.ru

Abstract—In the Arctic, global warming is 2−3 times faster than over other regions of the globe. As a result, noticeable changes are already being recorded in all areas of the environment. However, there is very little data on such changes in the Russian Arctic. Therefore, to fill the gap in the data on the vertical distribution of the gas and aerosol composition of air in this region, an experiment was carried out on the Tu-134 *Optik* laboratory aircraft in September 2020 to sound the atmosphere and water surface over the water areas of all seas in the Russian Arctic. This paper analyzes the spatial distribution of methane. It is shown that during the experiment its concentration was the highest over the Kara Sea (2090 ppb), the lowest over the Chukchi Sea (2005 ppb). The East Siberian and Bering seas were slightly different from the Chukchi Sea in terms of the methane concentration. Average values of CH_4 are characteristic of the Barents (2030 ppb) and the Laptev Seas (2040 ppb). The difference between the concentrations at an altitude of 200 meters and in the free troposphere attained 150 ppb over the Kara Sea, decreased to 91 and 94 ppb over the Barents and Laptev Seas, and further decreased over the East Siberian, Chukchi, and Bering Seas to 66, 63, and 74 ppb, respectively. Horizontal heterogeneity in the distribution of methane over the Arctic seas is the greatest over the Laptev Sea, where it attained 73 ppb. It is two times higher than over the Barents and Kara Seas, and 5−7 times higher than over the East Siberian and Bering Seas.

Keywords: Arctic, atmosphere, air, vertical distribution, methane, greenhouse gases, transport, impurities, composition

DOI: 10.1134/S1024856023050032

INTRODUCTION

One of the main problems classified by the world community as "great challenges" is global warming and the resulting environmental change. Predicted 40 years ago [1], it recently received another very strong confirmation in [2, 3]: all previous cooling and warming events in the time period from 0 to 2000 AD were regional, and the current one is global. However, there are regions where the warming occurs faster. The Arctic relates to these regions; the increase in air temperature is two to three times higher there than in other regions [4, 5]. This phenomenon is called the arctic amplification [6, 7]. In this regard, natural questions arise: how does warming in the Arctic affect the air composition [8−13] and how does it correlate with impurities entering the region [14−17]? Answering these questions, as well as drawing up a plan of measures to preserve the vulnerable Arctic nature, is possible only on the basis of measurements and analysis of direct and inverse relationships between the climate

warming and changes in the air composition [18]. However, such data for in the Russian Arctic are insufficient. As a result, there is a situation where irreversible environmental processes are taking place in the Arctic requiring immediate response, and the information about them is lacking, even estimates. Due to the lack of data from the Russian Arctic, a disappointing conclusion was drawn in [19] that environmental and socio-economic forecasts for the region under study are impossible.

Studies of the atmospheric composition in the Arctic are most often carried out in the surface air layer along the coast of the Arctic Ocean [20−27]. The data from such studies on the dynamics of aerosol and gas impurities in coastal areas make it possible to estimate the power of sources and sinks of impurities controlled. The processes of the exchange of impurities between ocean the water surface, which is becoming more and more free of ice, and the atmosphere remain unclear. There is no information on the vertical distri-

bution of impurities, which, as shown in the analysis of the heating of different air layers, is very important [28, 29]. Air heating can occur not only in the surface air layer, but also in the middle troposphere. This complicates the modeling of climate processes and greatly complicates the forecast of environmental changes.

Outside the Russian Arctic, laboratory aircraft are widely used to study the vertical distribution of gaseous and aerosol impurities [30–32]. The aircraft method for studying the atmospheric composition along the vertical is now recognized as reference [33], since it allows the use of precision instruments and measurements, including of the main meteorological parameters, with a good space and time referencing.

In the Russian Arctic, air composition was studied only in the surface (drift) air at drifting stations [34, 35] or from research vessels [36–42]. In 2010, a well-equipped Tiksi coastal international hydrometeorological observatory appeared [43], which, unfortunately, is the only one at the Arctic Ocean coast, which, is several thousand kilometers long in the Russian sector. In the past decade, the authors of this work carried out two small flight campaigns in the Russian Arctic within international projects [44, 45].

To fill the gap in the data on the vertical distribution of gaseous and aerosol compositions of the atmosphere, we carried out an experiment on sounding the atmosphere and water surface over all seas of the Arctic Ocean in the Russian Arctic (Barents, Kara, Laptev, East Siberian, and Chukchi) in September 2020 from the TU-134 *Optik* laboratory aircraft. The Bering Sea in the Pacific Ocean was chosen as reference in relation to the Arctic. It should be noted that such a large-scale experiment was not carried out either in the former Soviet Union or in modern Russia. The experiment and the parameters of the equipment used are described in [46]; average concentrations of impurities over all seas are also given there. The present work begins a series of papers with the detailed analysis of the air composition over each of seas.

Let us start this series from methane. The importance of studying the dynamics of this air component in the Arctic has recently dramatically increased due to the degradation of permafrost. The high concentrations of CH_4 over the region under study was ascertained both in the surface measurements [47, 48] and from satellite data [49, 50] for the tropospheric depth. However, opinions differ regarding how the methane concentration increases.

The methane emission from the ocean water surface into the atmosphere was numerically simulated with direct measurement data. The analysis of the simulation results has shown that the amount of CH_4 emitted is insufficient to form the concentrations observed [51–53].

Additional methane can come from the decomposition of gas hydrates on the ocean bed. This phenomenon was recorded, in particular, in measurements from sea vessels by researchers of the Far Eastern Branch of the Russian Academy of Sciences under the leadership of I.P. Semiletov [54–56]. However, there are scientists who disagree with the assessment made by Semiletov of the scale of the threat from the decomposition of gas hydrates [57, 58]. Moreover, it was found in recent works [59, 60] that there are no frozen rocks and gas hydrates in the areas where seeps were found, and the seeps are due to the migration of gases from great depths through the existing faults.

Some researchers believe that an additional amount of methane and other impurities can be transferred to the Arctic Ocean from the surrounding land [61–64], including from swamps, gas fields, and fires [39–42], and not only through air. The water in the Arctic Ocean comes from more southerly oceans, which carry an additional amount of microbes and bacteria [65]. They, in turn, can additionally emit a certain amount of methane into the atmosphere [66, 67]. The transfer of impurities to the Arctic turned out to be so significant, but little studied, that the German Aerospace Agency organized a special HALO-AC program, within which three laboratory aircraft are to simultaneously study this process at different altitudes [68].

The transfer is also possible from coastal areas where permafrost is actively thawing under conditions of the warming climate, in which a huge amount of organic matter is accumulated. It is processed by anaerobic microbes into methane or carbon dioxide [69–71]. Moreover, the reserves of organics are so large that they are called a delay action "hidden carbon bomb" [72], which can "explode" with further warming in the region.

In addition to methane emission from the soil, the thawing of permafrost in the Arctic results in the formation of thermokarst lakes, the release of methane from which is an order of magnitude more intense than from other sources and can attain hundreds of grams per square meter per year [73–76]. According to [77], the area of lakes in plains can occupy from 10 to 30% of such territories. Therefore, this source is comparable in power with others.

The recently published review on the budget of methane in the atmosphere [78] refines the power ranges of individual sources on the planet, but it does not answer the question about the reasons for the increase in the CH_4 concentration over the Arctic. Estimates of the CH_4 emission power of one or another source in [79] show that they can differ by three orders of magnitude. Their power is apparently growing. Methane concentrations rose more in 2021 than in any previous year, according to the US National Oceanic and Atmospheric Administration (NOAA), which summarized measurement data from 40 sites around the world. This once again emphasizes the importance of studying the spatiotemporal variability of methane in the atmosphere [80].
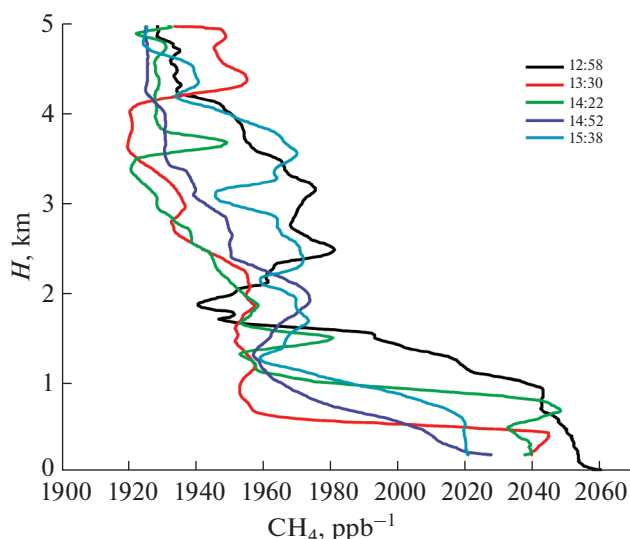
Fig. 1. Vertical distribution of the methane concentration over Arkhangelsk (12:58) and the Barents Sea (13:30, 14:22, 14:52, and 15:38) on September 4, 2020.

Since [46] gives a complete description of the experiment, we do not repeat it in this paper. We only recall that the methane concentration was measured with a G2301-m CRDS gas analyzer (Picarro Inc., United States). This device is designed specifically for laboratory aircraft and allows one to measure the CH_4 concentration in the range 0−20 ppm with an error < ± 0.0015 million^{-1} and a frequency of 1 Hz. The methane profiles were retrieved from the data of every second measurements using a moving average over 30 points and subsequent interpolation with an altitude step of 10 m.

The small differences in methane concentrations over different seas above 5000 m was also shown in [46]. Therefore, data above 5000 m are not considered in this work.

1. VERTICAL DISTRIBUTION

1.1. Barents Sea and Coastal Areas

The atmospheric sounding over the Barents Sea was carried out on September 4, 2020. It began with a climb in Arkhangelsk at 12:58 (hereinafter, GMT time). Then the aircraft twice descended to 200 m asl and twice ascendedup to 9000 m. One CH_4 concentration profile was derived over land and four over the sea (Fig. 1). Profiles are marked by their start time: 13:30, 14:22, 14:52, and 15:38 (sea); 12:58 (land).

Figure 1 shows that the methane concentrations were maximal in the mixing, surface, or near-water air layers. The vertical distribution of methane concentration in the troposphere was largely determined by the structure of the atmospheric boundary layer (ABL). The height of this layer (H_{ABL}) was estimated from

changes in the virtual potential temperature profiles (θ_v) (the data for the calculation of which were synchronously measured with the gas components), the mixing ratio (r), and the concentration of atmospheric impurities by the method [81]. Their dynamics are shown in Fig. 2. One can see that H_{ABL} varied from 1.5 to 2.3 km over land and most of the water area during the experiment. Attention should be paid to the large variation in the ABL height over different parts of the Barents Sea. The sites where the profiles were derived can be seen in Fig. 3b. Some profiles have secondary maxima in the lower part of the ABL. The difference between the concentrations in the surface (near-water) layer and the upper boundary of the ABL attains 110−140 ppb.

This vertical distribution of methane indicates that the main source of this gas is on the underlying surface, whether it be land or sea. The vertical sounding of the atmosphere was carried out after 16:00 local time, when the inner mixing layer had already disintegrated and, due to turbulent mixing, impurities began to propagate throughout the ABL [82]. Above the ABL, a slow decrease in the methane concentration is observed up to an altitude of 5000 m. This conclusion is also supported by the profiles of the mixing ratio of the water vapor (Fig. 2), the source of which is evaporation from the underlying surface.

Figure 1 shows that the CH_4 concentration in the ABL was higher over land than over the sea. Since, according to the analysis of the synoptic situation [46], air transport during this period occurred in a north-easterly direction, this can mean that the coastal sources of methane were of higher power than the marine source during that period. The back trajectories for that day shown in Fig. 3a also confirm this. They are constructed for the corner points of a "conditional" triangle representing the route of the Tu-134 *Optik* laboratory aircraft (red curve in Fig. 3b).

As can be seen from Fig. 3 the air that entered the region of measurements in the ABL was formed over the land. In the free troposphere, the transport direction changed from southwest to west.

In order to confirm that the power of the coastal sources was higher than that of the marine one, the differences between the concentrations over the sea and in the Arkhangelsk area are shown in Fig. 2f. One can see that the negative difference in the concentrations of CH_4 of up to 95 ppb is observed inside the ABL, near an altitude of 1000 m. It decreases towards the upper boundary of the ABL. At the level H_{ABL} it becomes positive, and in the middle troposphere it again becomes negative. Above 4000 m, the differences in concentrations become less significant.

Thus, it can be concluded that during the period of the experiment over the Barents Sea, the power of the coastal sources of methane was higher than over the water surface, i.e., the CH_4 was transported from land.
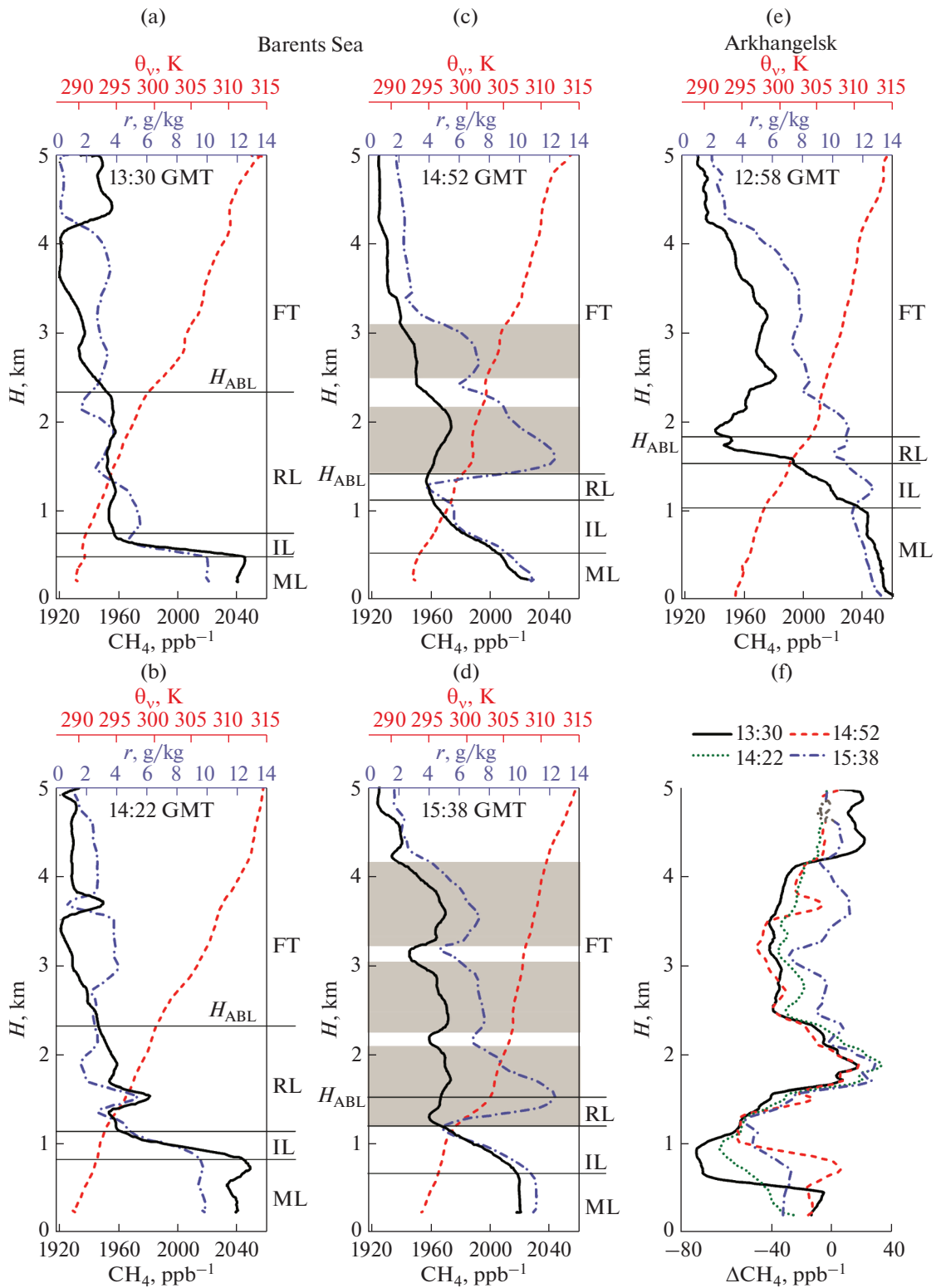
Fig. 2. Vertical distributions of the methane concentration (black curve), mixture ratios r (blue curve), and virtual potential temperature θ_v (red curve) (a−d) over the Barents Sea and (e) in the region of Arkhangelsk; (f) (land−sea) differences in the methane concentrations on September 4, 2020. Hereinafter in the figures: ML is the mixing layer, IL is the involvement layer, RL is the residual layer, FT is the free troposphere; cloud layers are shaded.
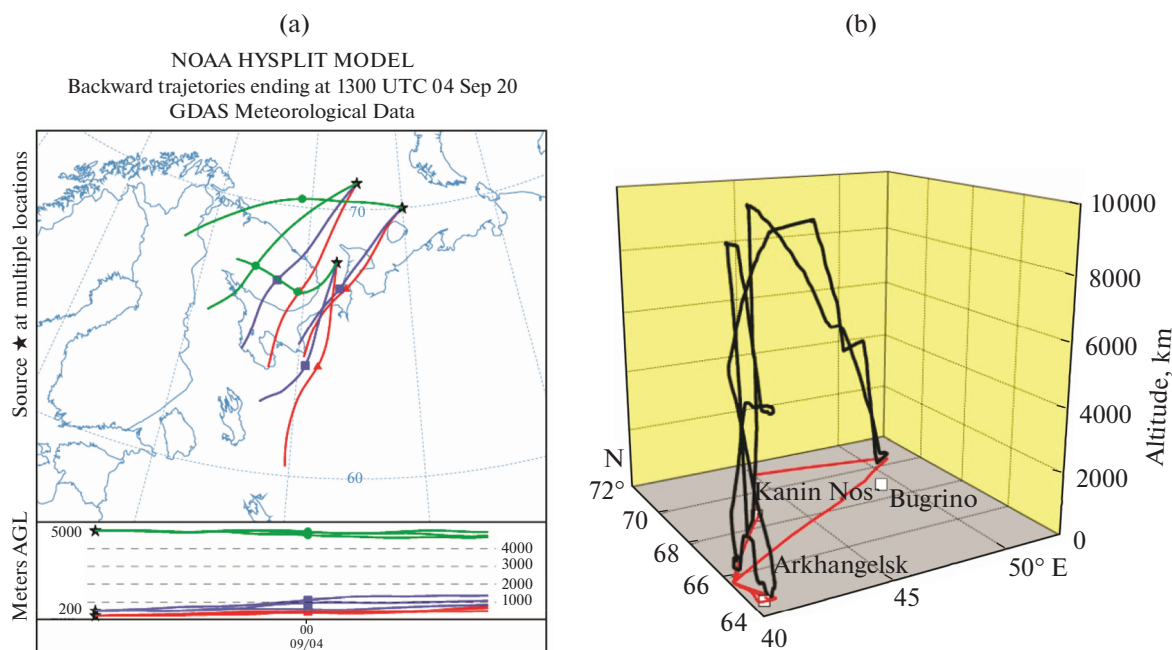
(a)

(b)

Fig. 3. (a) Back trajectories of air masses for the areas of measurement of vertical profiles of methane concentration (13:00–15:00 GMT, September 4, 2020); (b) pattern of the flight scheme to the Barents Sea area.

1.2. Kara Sea

The air composition over the Kara Sea was measured on September 6, 2020. The sounding was carried out according to a scheme whose horizontal projection is similar in shape to a hysteresis loop. The aircraft laboratory departed from the Naryan-Mar airport. Four vertical concentration profiles were measured over the sea (Fig. 4). A profile measured near Naryan-Mar region is added for comparison.
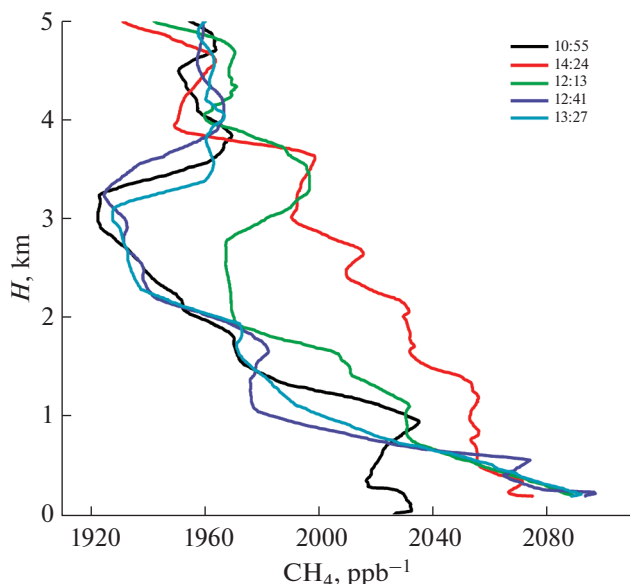

Fig. 4. Vertical distribution of the methane concentration over Naryan-Mar (10:55) and the Kara Sea (11:24, 12:13, 12:41, and 13:27), September 6, 2020.

According to profiles "11:24" and "12:13," the methane concentration is higher over the sea than over land not only in the surface and near-water layers, but also throughout the lower troposphere (up to 4000 m). The difference between the concentrations in the near-water layer (200 m) and the minimum value near an altitude of 3000 m attains 180 ppb. The retarding properties of the upper boundary of the ABL, the height of which is 1.8 km above the land and varied from 1.7 to 2.0 km above the sea, are not pronounced (Fig. 5).

This vertical distribution of methane in this region indicates that there is a source of CH_4 in the Kara Sea, which is of higher power than coastal sources. This is confirmed by the data in Fig. 6a, which shows the back trajectories for that day. It can be seen that air arrived to all areas of the Kara Sea where airborne sounding was carried out from the adjacent land along southwestern trajectories. Thus, a certain amount of methane emitted from the sea surface was added to the methane transported with the incoming air mass. The concentration of this additional methane attained ~80 ppb over the Kara Sea. Near an altitude of 1000 m, a thin layer was observed, where the methane content was less than over the mainland. An additional amount of methane again appears in the 1500–4000 m layer above certain areas of the Kara Sea, probably, due to the inhomogeneity of the methane emission from the ocean surface. We will dwell on this issue a little later.

Above 4000 m, the behavior of the concentrations (Fig. 5a–5e) and their differences (Fig. 5g) is neutral.
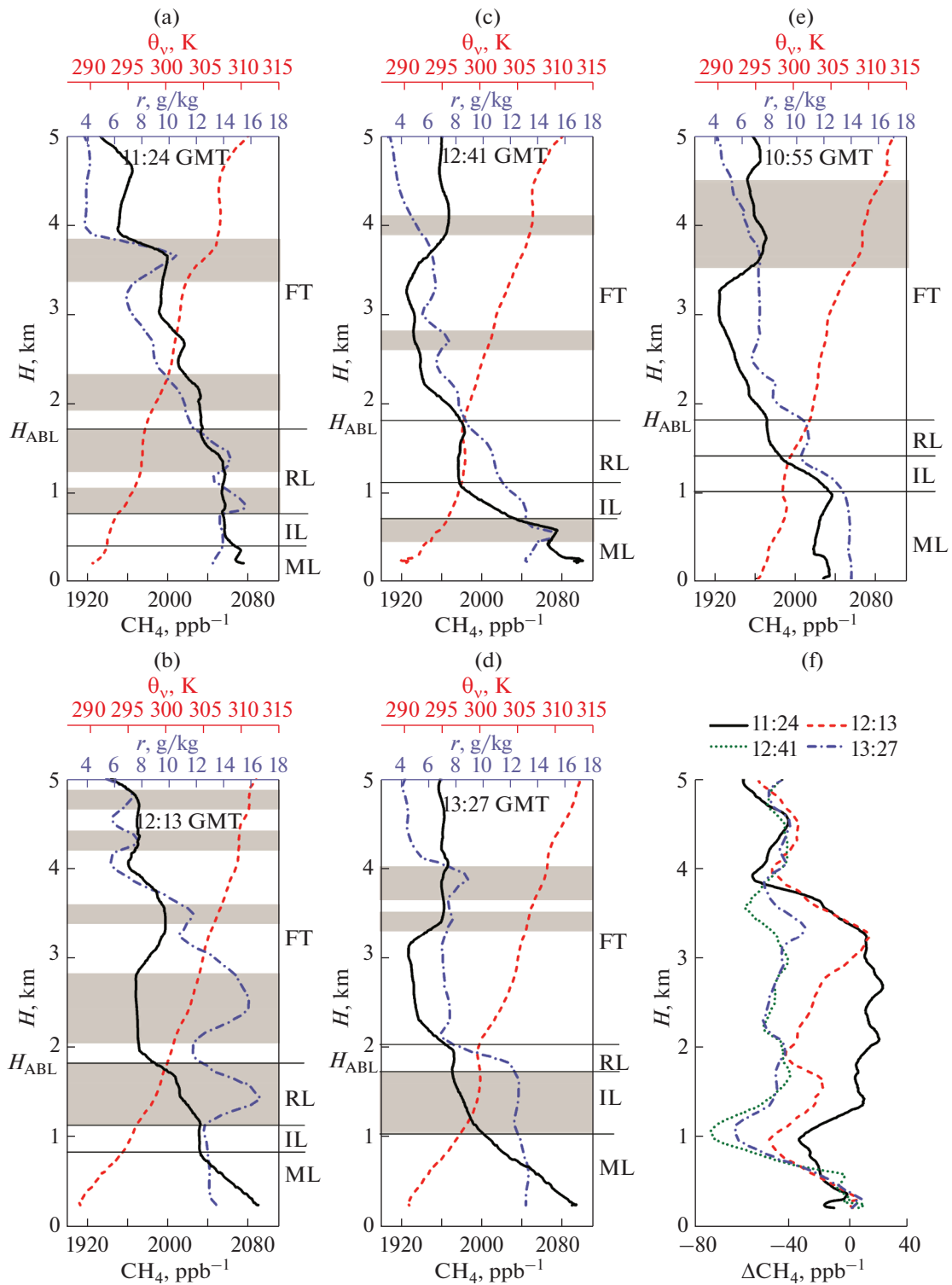
Fig. 5. Vertical distributions of the methane concentration (black curve), mixing ratios (blue curve), and virtual potential temperature (red curve) (a−d) over the Kara Sea and (e) in the Naryan-Mar region; (f) (land−sea) differences in methane concentrations on September 6, 2020.

1.3. Laptev Sea

The sounding over the Laptev Sea was carried out on September 9, 2020, starting from the Tiksi airport following the triangle scheme (Fig. 7).

The concentration of methane in this area is noticeably lower than in the previous ones. This indicates a lower power of CH_4 sources in the surrounding area and on the sea surface. At the same time, the con-
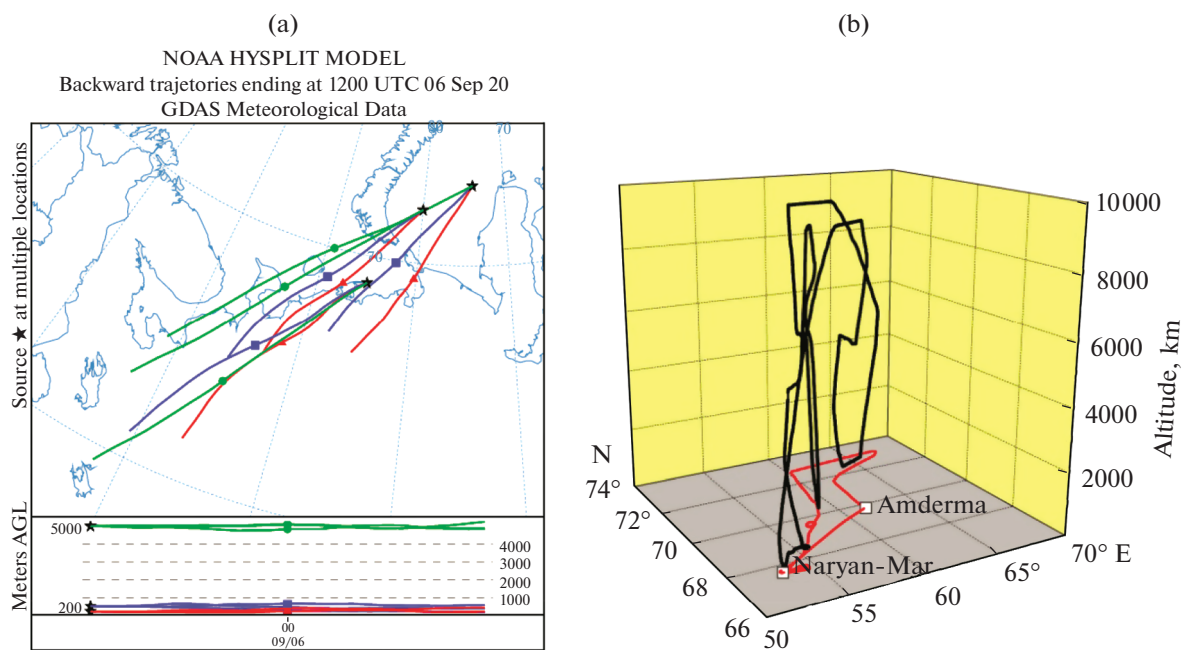
Fig. 6. (a) Back trajectories of air masses for the areas of measurements of the methane profiles (11:00−13:00 GMT, September 6, 2020); (b) pattern of the flight to the Kara Sea area.

tent of methane over the sea is higher than over land, both in the near-surface (drift) layer and in the lower troposphere as a whole. The difference between the concentrations in the near-water layer and the lower troposphere also decreased, it is less than 100 ppb here.

The nature of the vertical distribution of methane concentration noticeably changes over the territory under study. It depends on the height of the mixing

Fig. 7. Vertical distribution of the methane concentration over Tiksi (03:09) and the Laptev Sea (03:42, 04:21, 04:50, and 05:30) on September 9, 2020.

layer, which varied from 200 to 700 m (Fig. 8). Secondary concentration maxima are seen in the residual ABL layer. This situation has developed due to the peculiarities of air transport in the region under study. Air was supplied to the water area of the Laptev Sea from the western regions of the Arctic Ocean, and to Tiksi, on the contrary, from the continental regions. In this case, it is difficult to assume a relationship between the methane concentrations over the land and sea. Therefore, a land−sea comparison is omitted.
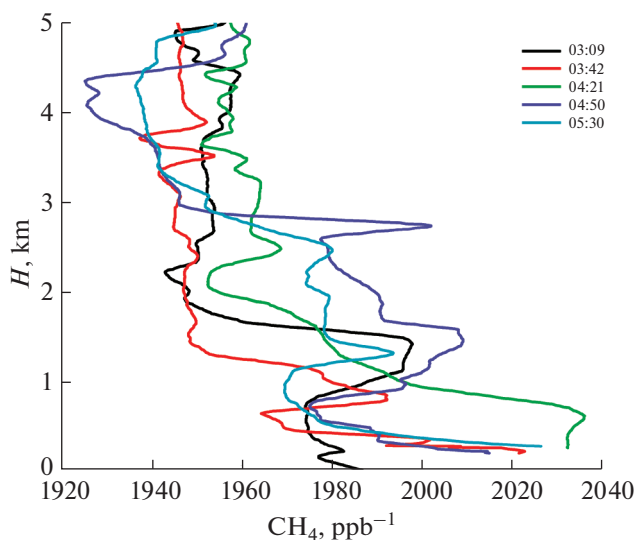
1.4. East Siberian Sea

Due to the fact that the Pevek airport was closed for repairs, sounding of the atmosphere over the East Siberian and Chukchi Seas was started from the Anadyr airport. The flight to and departure from the sounding site took a lot of time and reduced the time of the main work. As a result, the territory under study was smaller. Nevertheless, we revealed the features of the methane distribution over these seas (Figs. 9 and 10).

Figure 9 shows that the vertical methane distribution over the East Siberian Sea generally corresponds to the previous profiles. The highest concentrations are observed in the near-surface air layer, then the concentration drops up to an altitude of 2500 m. Above, the behavior was close to neutral. In contrast to the distributions over the western seas, the change to the neutral behavior occurs much lower here. Over the western seas, it was observed near and above 4000 m. This difference is due to the low height of the mixing layer, which did not exceed 1000 m in four of the five
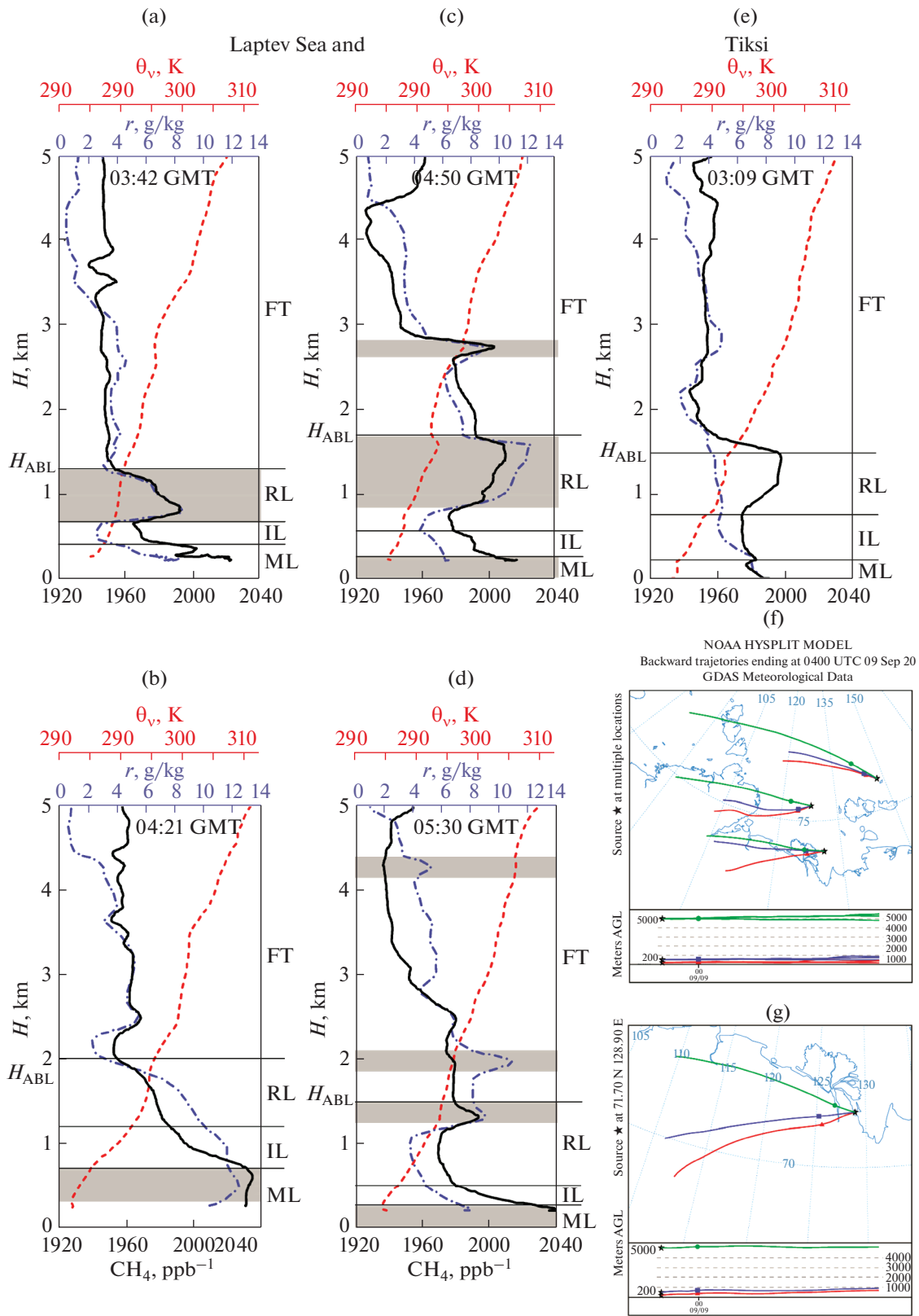
Fig. 8. Vertical distributions of the methane concentration (black curve), mixing ratio (blue curve), and virtual potential temperature (red curve) (a–d) over the Laptev Sea and (e) in the Tiksi region; back trajectories of air masses for areas of measurements of the methane profiles over (f) the Laptev Sea and (g) Tiksi (03:00–05:00, September 9, 2020).
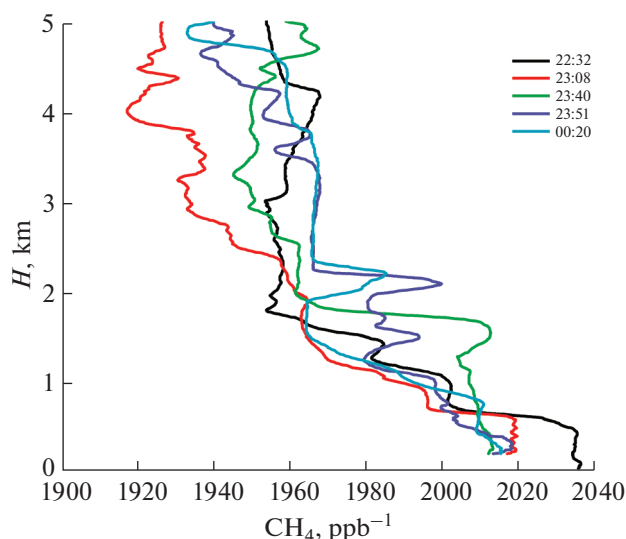
Fig. 9. Vertical distribution of the methane concentration over Anadyr (22:32) and the East Siberian Sea (23:08, 23:40, 23:51, and 00:22) on September 15−16, 2020.

profiles (Fig. 10). The difference between the concentrations in the near-water layer and in the lower troposphere also significantly lower, 84 ppm. One can also note a smaller spread of concentrations between individual profiles at all altitudes. This indicates the homogeneity of the methane source in the air mass entering the sea area.

This vertical distribution is explained by the history of the air mass observed in the area of the experiment. As follows From Fig. 10f the air in the near-water and boundary layers came from the Western Hemisphere, from the Arctic Ocean surface along the Alaska coastline. In the free troposphere, the air was also transferred from the Arctic Ocean. Since measurements were not made in those areas, a comparison cannot be made.

1.5. Chukchi Sea

The sounding over the Chukchi Sea was carried out on September 14−15, 2020, a day earlier than over the East Siberian Sea, due to synoptic conditions. The measurement data are shown in Fig. 11.

The comparison between Figs. 7 and 11 shows that the nature of the vertical distribution and the methane concentration over the Chukchi Sea is close to that observed over the East Siberian Sea. But the change to the neutral behavior of the concentration occurred even lower, near an altitude of 1800 m, over the Chukchi Sea,. The mixing layer was located noticeably lower here, at an altitude of no more than 600 m (Fig. 12).

The CH_4 concentration in the ABL above the sea surface was higher than above the continent. This comparison is conventional, since the territory between the Chukchi Sea and Anadyr is mountainous, and the

mountains prevents the transfer of air masses. The maximal difference in the concentrations is 85 ppb.

Air arrive to the water area of the Chukchi Sea in the ABL through the Pacific Ocean from the territory of Alaska (Fig. 12f). In the free atmosphere, the was air arrived from the Pacific Ocean, but bypassing Alaska.

1.6. Bering Sea

Sounding over the Bering Sea was not scheduled. However, the peculiarities of methane distribution over the East Siberian and Chukchi Seas necessitated a control flight, because of the large differences between the methane concentration in the near-air layer over the western and eastern seas. The measurements were taken on September 16, 2020, in the afternoon. The aircraft flew from the Anadyr airport immediately towards the Bering Sea at a low altitude. Fig. 8e shows the profile measured in the Anadyr region two hours earlier, when returning from the East Siberian Sea.

The data in Fig. 13 repeat the measurements over the East Siberian and Chukchi Seas both in terms of methane concentrations and of the boundary of the change to neutral altitude variations. The difference between the concentrations in the near-water layer and in the lower troposphere remained the same, 83 ppb on average. The height of the mixing layer over the Bering Sea was close to that observed over the East Siberian and Chukchi Seas, and the height of the ABL increased as compared to the Chukchi Sea (Fig. 14).

In contrast to the profiles over the previously considered seas, the profiles in Figs. 13 little differ from each other over different parts of the Bering Sea in the ABL. Differences are mainly observed above H_{ABL}. This is due to the peculiarities of air transport at these altitudes. Figure 14f shows that the air mass trajectories are similar to those over the Chukchi Sea, which causes the noticeable difference between the methane concentrations in the free troposphere.

2. HORIZONTAL INHOMOGENEITIES IN THE METHANE DISTRIBUTION

During the experiment, in addition to vertical sounding, horizontal flights were also performed at altitudes of 200, 5000, and 9000 m over different parts of the seas. During such flights, the concentrations of trace atmospheric gases were recorded at a frequency of 1 Hz. These data make it possible to estimate the variability of methane concentration over different parts of each sea. The areas where measurements were taken at an altitude of 200 m are shown in Fig. 15. We believe that, the inhomogeneity of the CH_4 emission from the ocean surface should be pronounced at this altitude. The measurement results are shown in Fig. 16 and allow the comparison between variations in the methane concentration over different seas.
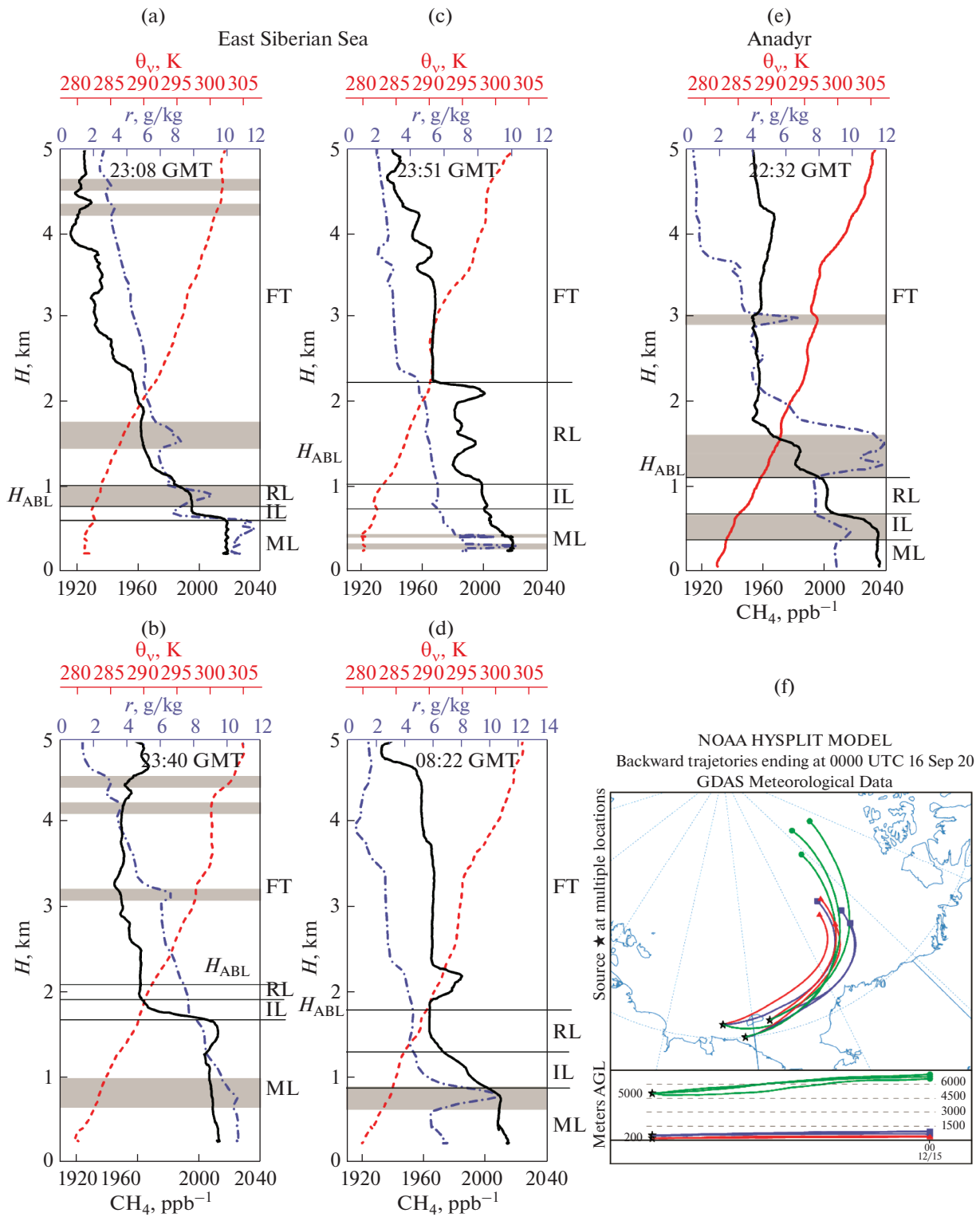
Fig. 10. Vertical distributions of the methane concentration (black curve), mixing ratio (blue curve), and virtual potential temperature (red curve) (a–d) over the East Siberian Sea and (e) in the Anadyr region; (f) back trajectories of air masses for areas of measurements of methane profiles over the East Siberian Sea (03:00–05:00, September 15–16, 2020).
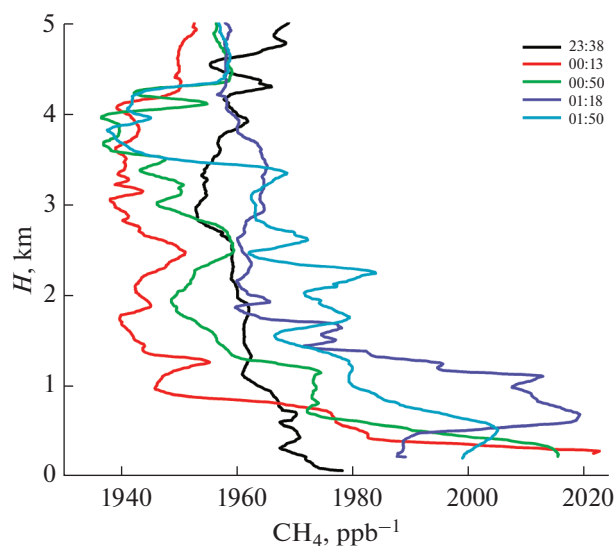
Fig. 11. Vertical distribution of the methane concentration over Anadyr (23:38) and the Chukchi Sea (00:13, 00:50, 01:18, and 01:50) on September 14−15, 2020.

On the one hand, Fig. 16 shows the differences in the methane concentrations over different seas noted in the previous section. On the other hand, it shows the features of their horizontal distribution over water areas. One can see that the variation in the CH_4 concentration is the highest over the Laptev Sea, up to 73 ppb in three sections with a total length of about 250 km. Over the Barents and Kara Seas, it exceeds 30 ppb. The smallest horizontal variations in the concentration were recorded over the East Siberian and Bering Seas. Now it is difficult to comment on these data. Perhaps, the cause is the geological structure of the sea bottom, which was reported in [59, 60]. Thus, five mesoscale structures are clearly visible over the Barents Sea, apparently reflecting the methane emission from the ocean surface. Fluctuations in the CH_4 concentration, but with shorter periods, also take [lace

over the Kara Sea. Perhaps this strong variability over the Laptev Sea is due to the presence of methane seeps described in [54−56].

3. DISCUSSION

The vertical profiles of CH_4 concentration measured in the experiment described are in good agreement with the data in other sectors of the Arctic acquired by foreign colleagues [83, 84]. The comparison of absolute values is unfair, since the methane concentration has a long-term trend, and our data do not coincide in time with measurements by other researchers.

To compare the methane concentrations in the near-water layer over different seas, Table 1 is compiled. It shows that the methane concentration at an altitude of 200 m averaged over all measurements was the highest over the Kara Sea (2091 ppb) and the smallest over Chukchi Sea (2005 ppb) during the experiment. Average values of the CH_4 concentration are characteristic of the Barents (2030 ppb) and the Laptev Seas (2022 ppb). The methane concentrations over the Laptev Sea and the East Siberian Sea (2015 billion^{-1}) slightly differ. The estimates obtained are partly confirmed by the results of works [85−87], where high methane concentrations were recorded over the Barents and Kara Seas.

The difference between the concentrations at an altitude of 200 m and in the free troposphere attained 180 ppb over the Kara Sea, decreased to 140 and 94 ppb over the Barents and Laptev Seas and decreased even more over the East Siberian, Chukchi, and Bering Seas: to 84, 85, and 83 ppb, respectively. This reflects the emission characteristics of the seas. Partial confirmation of our data can be the measurements of methane fluxes in the near-water layer [88], where the annual methane fluxes in the Laptev, East Siberian, and Chukchi Seas are estimated as 0.83; 0.62, and 0.03 Tg/year, respectively.

The difference in the concentrations weakly depends on the height of the ABL and water and air

Table 1. Average characteristics of methane distribution and its variability and measurement conditions

| Parameter	Sea					
	Barents	Kara	Laptev	East Siberian	Chukchi	Bering
CH_4 concentration at an altitude of 200 m, ppb	2030 ± 11	2091 ± 6	2022 ± 16	2015 ± 2	2005 ± 13	2012 ± 3
ABL height, km	1.9 ± 0.5	1.8 ± 0.1	1.6 ± 0.3	1.8 ± 0.5	1.3 ± 0.3	1.7 ± 0.2
Difference between methane concentrations at 200 m and in the free troposphere, ppb	140	180	94	84	85	83
Air temperature at an altitude of 200 m, °C	14.7 ± 1.9	12.1 ± 0.6	7.2 ± 1.7	3.6 ± 0.4	5.0 ± 0.4	6.9 ± 0.3
Sea temperature (coastal stations), °C	11	8	7	5	4	8
Range of variation in the methane concentrations at an altitude of 200 m in horizontal sections, ppb	32	36	73	10	23	13
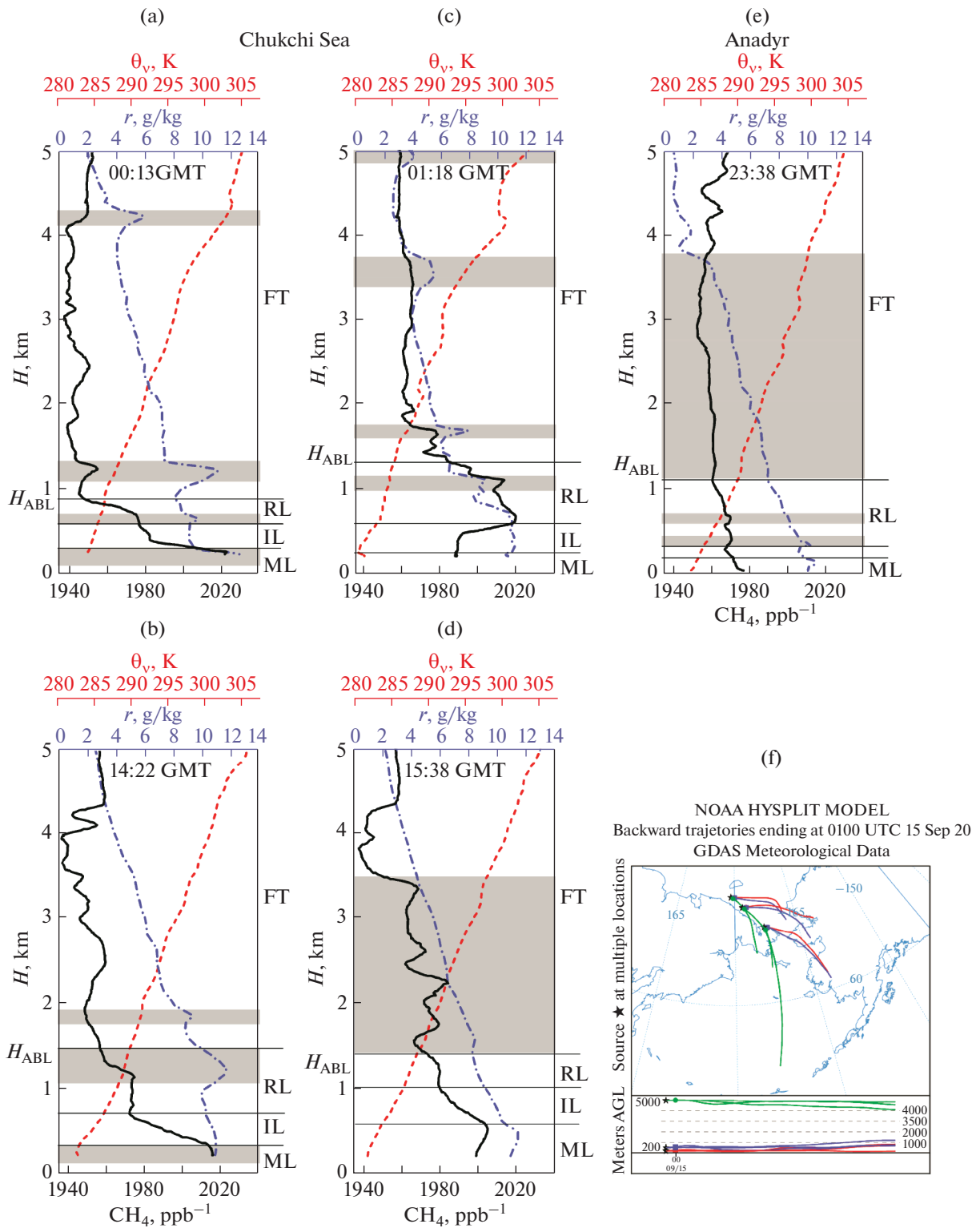
Fig. 12. Vertical distributions of the methane concentration (black curve), mixing ratio (blue curve), and virtual potential temperature (red curve) (a−d) over the Chukchi and (e) in the Anadyr region (e); (f) back trajectories of air masses for areas of measurements of methane profiles over the Chukchi Sea (00:00−02:00, September 14−15, 2020).
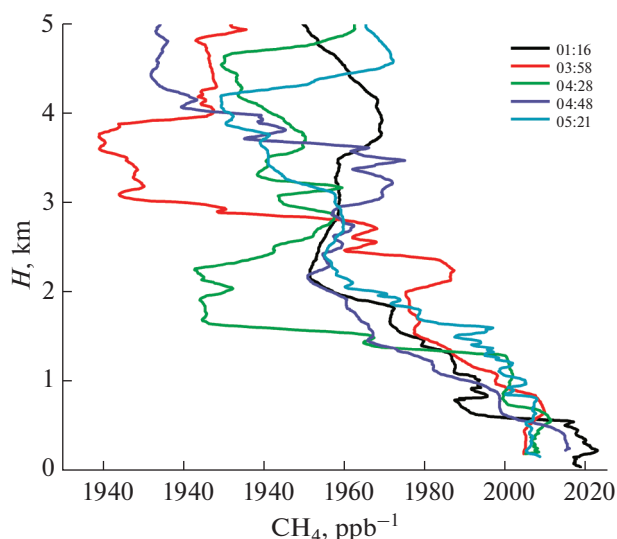
Fig. 13. Vertical distribution of the methane concentration over Anadyr (01:16) and the Bering Sea (03:58, 04:28, 04:48, and 05:21) on September 16, 2020.

temperatures (see Table 1). It is possible that internal mixing requires more time over the sea [82] than over land, so methane faster penetrates into the free troposphere over land.

Many works (for example, [89–93]) state that coastal areas emit more methane than the ocean. This is not about catastrophic processes [94, 95]. The source of methane on land is probably thermokarst lakes, which formed in abundance in the coastal tundra. The above data shows that there are cases where the CH_4 concentration is higher over land than over sea, and vice versa. It should be emphasized here that the flights over the seas were carried out in the daytime, when the inner mixing layer was absent and the processes of impurity accumulation were not observed. They can make a significant contribution over land. To estimate the possible power of the sources, we have compiled Table 2, which contains the maximal concentrations of methane over the seas and coastal areas during the experiment. One can see that the maximal methane concentrations during the experiment were

Table 2. Maximum methane concentrations over the seas and coastal areas, ppb

Sea	CH_4	Shore	CH_4
Barents	2046	Arkhangelsk	2092
Kara	2104	Naryan-Mar	2203
Laptev	2054	Tiksi	2061
East Siberian	2020	Anadyr	2038
Chukchi	2021	Anadyr	2038
Bering	2018	Anadyr	2038

higher over coastal regions than over sea areas. This is because CH_4 accumulates in the inner mixing layer at night in the presence of local sources. In the first half of the day, when the inner mixing layer is destroyed [82], the gas spread throughout the ABL. This is clearly seen from the CH_4 profiles in Fig. 17. During 10 hours that passed between two soundings, the methane concentration in the inner mixing layer (0–500 m) increased from 2065 to 2200 ppb^{-1}, i.e., by 135 ppb. Above 500 m, CH_4 concentration varied much weaker. The usual air masses speed is 30–50 km/h [96]. Hence, an air mass could be transported to 300–500 km for 10 hours. Hence, it is quite obvious that the increase in methane concentration occurred due to emissions from local sources located near the measurement site. If the total transfer is directed towards the ocean, then the additional amount of methane will be transferred there.

CONCLUSIONS

The analysis of the vertical distribution of methane over all the Arctic seas showed that its concentrations were maximal in the surface or surface air layer during the experiment. Some profiles have secondary maxima in the lower part of the ABL. The difference between the concentrations at a level of 200 m and in the free troposphere attained 180 ppb over the Kara Sea and decreased to 84, 85, and 83 ppb, respectively, over the East Siberian, Chukchi, and Bering Seas This vertical distribution of methane indicates that the main source of this gas is on the underlying surface, whether it be land or sea, and reflects the emission characteristics of the seas. Above the upper boundary of the ABL, the methane concentration gradual decreased up to an altitude of 5000 m.

The comparison between the methane concentrations at an altitude of 200 m over all seas showed that it was maximal over the Kara Sea and minimal over the Chukchi Sea. The East Siberian and Bering Seas slightly differed from the Chukchi Sea. The Barents and Laptev Seas occupy an intermediate position. Such a difference in the methane distribution in this region indicates that there is probably a source of CH_4 in the Kara Sea, which is of higher power than the others. In this case, the concentration difference weakly depends on the height of the ABL and the water and air temperatures.

The comparison of the methane concentrations over the sea and land at the same altitude revealed that the concentration was higher over the coastal area than over the sea in the Barents Sea area. It decreased with the distance from the coast. In the Kara Sea region, on the contrary, the concentration noticeably increased with the distance from the coast. The "land–sea" difference in the CH_4 concentrations was zero in the area of the Laptev Sea. The assessment of this difference for the rest of the seas with respect to the data for Anadyr showed a slight excess of methane concentra-
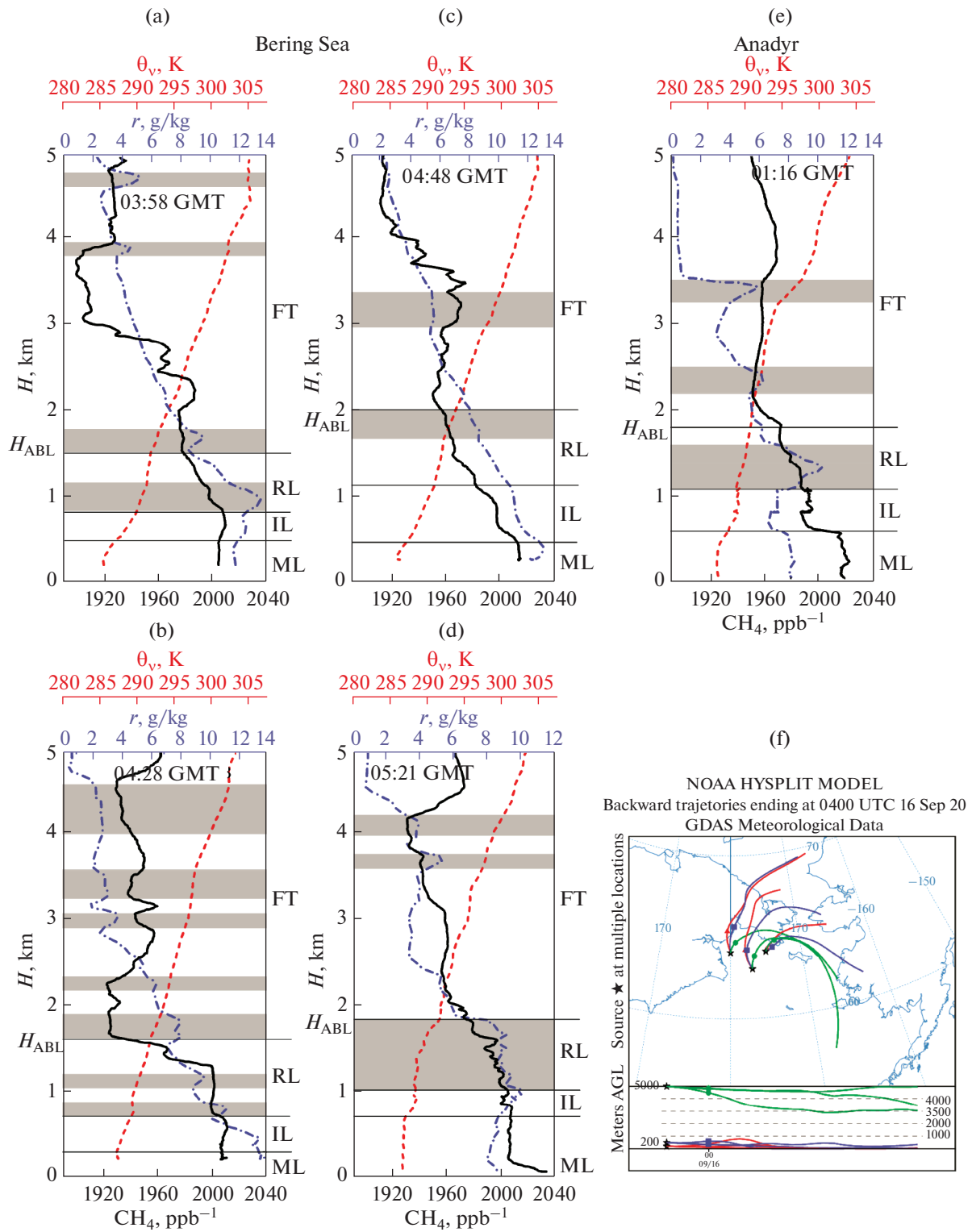
Fig. 14. Vertical distributions of methane concentration (black curve), mixing ratio (blue curve), and virtual potential temperature (red curve) (a−d) over the Bering Sea and (e) in the Anadyr region; (f) back trajectories of air masses for areas of measurements of methane profiles over the Bering Sea (04:00−05:00, September 16, 2020).
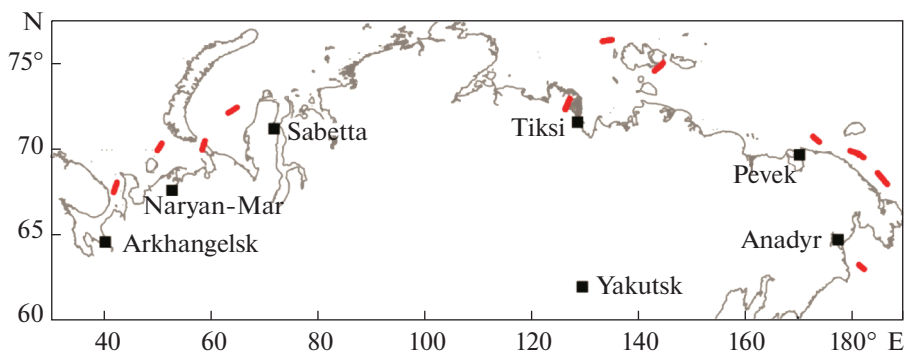
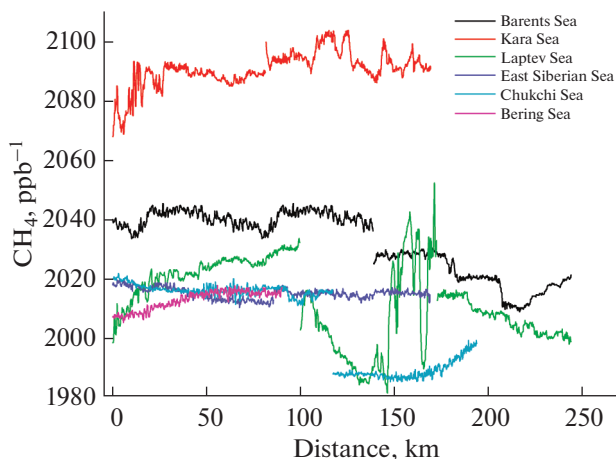**Fig. 15.** Areas (red lines) where methane concentrations were measured.

Fig. 16. Methane concentration at an altitude of 200 m above the seas of the Russian Arctic.
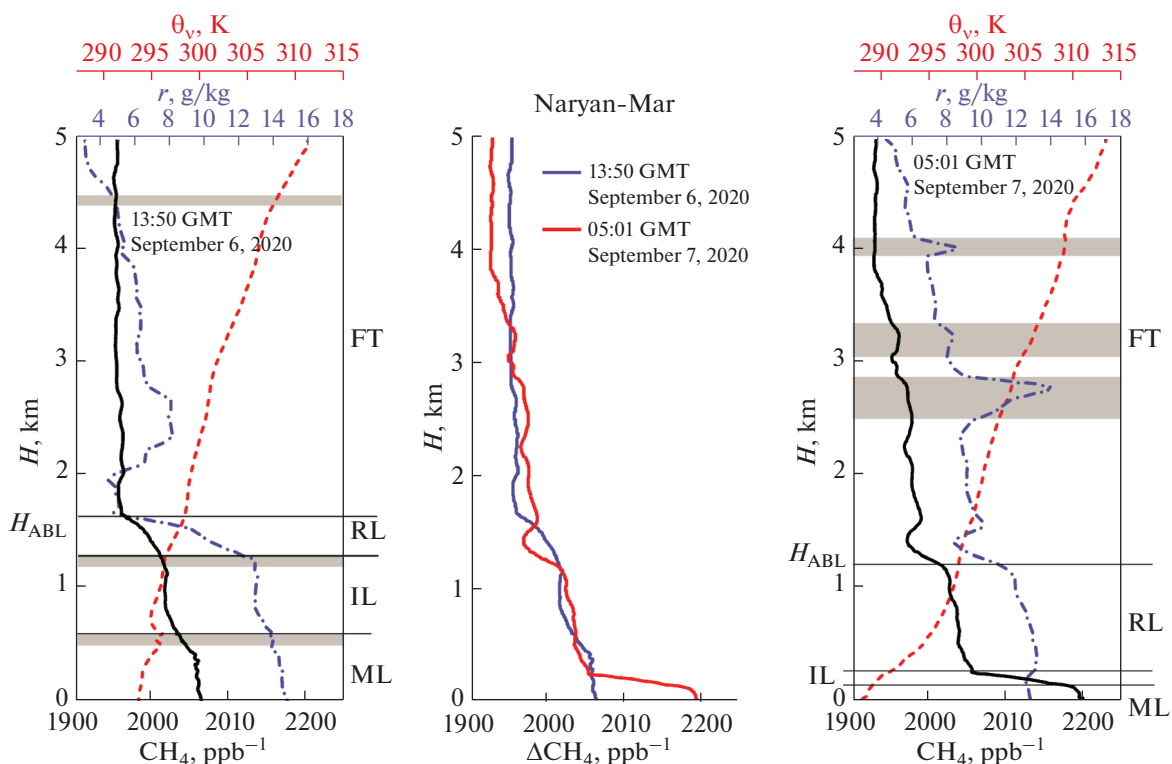

Fig. 17. (b) Vertical profiles of the methane concentration obtained in the Naryan-Mar region; (a, c) methane concentrations (black curve), mixture ratios (blue curve), and virtual potential temperature (red curve) on September 6 and 7, 2020.

tions over land. The comparison of the maximal methane concentrations recorded during the experiment over the seas and adjacent continental territories revealed that they were everywhere higher over land.

Taking into account the fact that the experiment was local in time, it should be emphasized that it is impossible to draw final conclusions either about the position of methane sources in the territory under study or about their intensity from the results. Further regular and systematic monitoring of atmospheric methane (and other greenhouse gases) is required.

CONFLICT OF INTEREST

The authors declare that they have no conflicts of interest.

REFERENCES

1. M. McNutt, "Times's up, CO_2," Science **365** (6432), 411 (2019).

2. S. S. George, "Aberrant synchrony of present-day warming," Nature **571** (7766), 481−482 (2019).

3. R. Neukom, N. Steiger, J. J. Gomez-Navarro, J. Wang, and J. P. Werner, "No evidence for globally coherent warm and cold periods over the preindustrial common era," Nature **571** (7766), 550−554 (2019).

4. T. G. Shepherd, "Effects of a warming Arctic," Science **353** (6303), 989−990 (2016).

5. M. R. Najafi, F. W. Zwiers, and N. P. Gillett, "Attribution of Arctic temperature change to grenhouse-gas and aerosol influences," Nat. Clim. Change **5** (3), 246−249 (2015).

6. V. A. Semenov, "Modern Arctic climate research: Progress, change of concepts, and urgent problems," Izv., Atmos. Ocean. Phys. **57** (1), 18−28 (2021).

7. A. V. Klepikov and A. I. Danilov, "Results of Russian studies of polar meteorology in 2015−2018," Izv., Atmos. Ocean. Phys. **57** (3), 233−246 (2021).

8. L. Travnik, "Carbon cycling in the Arctic," Science **345** (6199), 870 (2014).

9. R. M. Cory, C. P. Ward, B. C. Crump, and G. W. Kling, "Sunlight controls water column processing of carbon in Arctic fresh waters," Science **345** (6199), 925−928 (2014).

10. M. Sand, T. K. Berntsen, K. von Salzen, M. G. Flanner, J. Langner, and D. G. Victor, "Response of Arctic temperature to changes in emissions of short-lived climate forcers," Nat. Clim. Change **6** (3), 286−289 (2015).

11. D. Nomura, M. A. Granskog, A. Fransson, M. Chierici, A. Silyakova, K. I. Ohshima, L. Cohen, B. Delille, S. R. Hudson, and G. S. Dieckmann, "CO_2 flux over young and snow-covered Arctic pack ice in winter and spring," Biogeosci. **15** (11), 3331−3343 (2018).

12. S. Yasunaka, A. Murata, E. Watanabe, M. Chierici, A. Fransson, S. van Heuven, M. Hoppema, M. Ishii, T. Johannessen, N. Kosugi, S. K. Lauvset, J. T. Mathis, S. Nishino, A. M. Omar, A. Olsen, D. Sasano, T. Takahashi, and R. Wanninkhof, "Mapping of the air−sea CO_2 flux in the Arctic Ocean and its adjacent seas: Basin-wide distribution and seasonal to interannual variability," Polar Sci., No. 3, 323−334 (2016).

13. M. D. Willis, R. W. Leaitch, and J. P. D. Abbatt, "Processes controlling the composition and abundance of Arctic aerosol," Rev. Geophys. **56** (4), 621−671 (2018).

14. S. R. Arnold, K. S. Law, C. A. Brock, J. L. Thomas, S. M. Starkweather, K. Salzen, A. Stohl, S. Sharma, M. T. Lund, M. G. Flanner, T. Petaja, H. Tanimoto, J. Gamble, J. E. Dibb, M. Melamed, N. Johnson, M. Fider, V.-P. Tynkkynen, A. Baklanov, S. Eckhardt, S. A. Monks, J. Browse, and H. Bozem, "Arctic air pollution: Challenges and opportunities for the next decade," ELEMENTA: Sci. Atmos., No. 4, 16 (2016).

15. K. S. Law, A. Stohl, P. K. Quinn, C. A. Brock, J. F. Burkhart, J. D. Paris, G. Ancellet, B. Singh, A. Roiger, and H. Schlager, "Arctic air pollution," BAMS **95** (12), 1873−1895 (2014).

16. A. Roiger, J.-L. Thomas, H. Schlager, K. S. Law, J. Kim, A. Schafler, B. Weinzierl, F. Dahlkotter, I. Krisch, L. Marelle, A. Minikin, J.-C. Raut, A. Reiter, M. Rose, M. Scheibe, P. Stock, R. Baumann, C. Clerbaux, M. George, T. Onishi, and J. Flemming, "Quantifying emerging local anthropogenic emissions in the Arctic region," BAMS **96** (3), 441−460 (2015).

17. N. Evangeliou, Y. Balkanski, W. M. Hao, A. Petkov, R. P. Silverstein, R. Corley, B. Nordgren, S. P. Urbanski, S. Eckhardt, A. Stohl, P. Tunved, S. Crepinsek, A. Jefferson, S. Sharma, J. K. Njgaard, and H. Skov, "Wildfires in Northern Eurasia affect the budget of black carbon in the Arctic—a 12-year retrospective synopsis (2002−2013)," Atmos. Chem. Phys. **16** (12), 7587−7604 (2016).

18. M. Kulmala, T. Nieminen, R. Chellapermal, R. Makkonen, J. Back, and V.-M. Kerminen, "Climate feedbacks linking the increasing atmospheric CO_2 concentration, BVOC emissions, aerosols and clouds in forest ecosystems, " in *Biology, Controls and Model Tree Volatile Organic Compound Emissions*, Ed. by U. Niinemets and R.K. Monson (Springer, Dordrecht, 2010).

19. J. Schmale, S. R. Arnold, K. S. Law, T. Thorp, S. Anenberg, W. R. Simpson, J. Mao, and K. A. Pratt, "Local Arctic air pollution: A neglected but serious problem," Earth's Future, No. 6 (2018). https://doi.org/10.1029/2018EF000952

20. M. D. Willis, J. Burkart, J. L. Thomas, F. Kollner, J. Schneider, H. Bozem, P. M. Hoor, A. A. Aliabadi, H. Schulz, A. B. Herber, W. R. Leaitch, and J. D. Abbatt, "Growth of nucleation mode particles in the sum-

mertime Arctic: A case study," Atmos. Chem. Phys. **16** (12), 763−767 (2016).

21. E. Asmi, V. Kondratyev, D. Brus, T. Laurila, H. Liha-vainen, J. Backman, V. Vakkari, M. Aurela, J. Hatakka, Y. Viisanen, T. Uttal, V. Ivakhov, and A. Makshtas, "Aerosol size distribution seasonal characteristics," Atmos. Chem. Phys. **16** (13), 1271−1287 (2016).

22. A. E. Cassidy, A. Christen, and Y. R. Henry, "The effect of a permafrost disturbance on growing-season carbon-dioxide fluxes in high Arctic tundra ecosystem," Biogeosci. **13** (8), 2291−2303 (2016).

23. I. B. Strachan, R. A. Nugent, S. Crombie, and M. C. Bonneville, "Carbon dioxide and methane exchange at a cool-temperate freshwater marsh," Environ. Res. Lett. **10** (10), 10 (2015).

24. J. B. Fisher, M. Sikka, W. C. Oechel, D. N. Huntzinger, J. R. Melton, C. D. Koven, A. Ahlstrom, M. A. Arian, I. Baker, J. M. Chen, P. Ciais, C. Davidson, M. Dietze, B. El-Marsi, D. Hayes, C. Huntingford, A. K. Jain, P. E. Levy, M. R. Lomas, B. Poulter, D. Price, A. K. Sahoo, K. Schaefer, H. Tian, E. Tomelleri, H. Verbeeck, N. Viovy, R. Wania, N. Zeng, and C. E. Miller, "Carbon cycle uncertainty in the Alaskan Arctic," Biogeosci. **11** (15), 4271−4288 (2014).

25. M. Langer, S. Westermann, K. W. Anthony, K. Wischnewski, and J. Boike, "Frozen ponds: Production and storage of methane during the Arctic winter in a lowland tundra landscape in northern Siberia, Lena," Biogeosci. **12** (4), 977−990 (2015).

26. M. Giamarelou, K. Eleftheriadis, S. Nyeki, K. Torseth, and G. Biskos, "Indirect evidence of the composition of nucleation mode atmospheric particles in the high Arctic," J. Geophys. Res.: Atmos. **121** (2), 965−975 (2016).

27. C. L. Myhre, B. Ferre, M. Platt, A. Silyakova, O. Hermansen, G. Allen, I. Pisso, N. Schmidbauer, A. Stohl, J. Pitt, P. Jansson, J. Greinert, C. Percival, A. M. Fjaeraa, S. J. O'Shea, M. Gallagher, M. L. Breton, K. N. Bower, S. J. B. Bauguitte, S. Dalsoren, S. Vadakkepuliyambatta, R. E. Fisher, E. G. Nisbet, D. Lowry, G. Myhre, J. A. Pyle, M. Cain, and J. Mienert, "Extensive release of methane from Arctic seabed west of Svalbard during summer 2014," Geophys. Rev. Lett. **43** (9), 4624−4631 (2016).

28. A. Kylling, G. C. D. Zwaaftink, and A. Stohl, "Mineral dust instantaneous radiative forcing in the Arctic," Geophys. Rev. Lett. **45** (9), 4290−4298 (2018).

29. T. B. Zhuravleva, M. V. Panchenko, V. S. Kozlov, I. M. Nasrtdinov, V. V. Pol'kin, S. A. Terpugova, and D. G. Chernov, "Model estimates of dynamics of the vertical structure of solar absorption and temperature effects under background conditions and in extremely smoke-laden atmosphere according to data of aircraft observations," Atmos. Ocean. Opt. **31** (1), 24−30 (2018).

30. J. L. France, M. Cain, R. E. Fisher, D. Lowry, G. Allen, S. J. O. Shea Iii, J. Pyle, N. Warwick, B. T. Jones, M. W. Gallagher, K. Bower, M. L. Breton, C. Percival, J. Muller, A. Wellpott, S. Bauguitte, C. George, G. D. Hayman, A. J. Manning, C. L. Myhre, M. Lanoiselle, and E. G. Nisbet, "Measurements of $\delta^{13}C$ in CH_4 and using particle dispersion modeling to characterize sources of Arctic methane within an air mass," J. Geophys. Res. Atmos. **121** (23), 14257−14270 (2016).

31. B. Quennehen, A. Schwarzenboeck, J. Schmale, J. Schneider, H. Sodemann, A. Stohl, G. Ancellet, S. Crumeyrolle, and K. S. Law, "Physical properties of pollution aerosol particles transported from North America to Greenland as measured during the POLARCAT summer campaign," Atmos. Chem. Phys. **11** (21), 10947−10963 (2011).

32. W. R. Leaitch, A. Korolev, A. A. Aliabadi, J. Burkart, M. D. Willis, J. P. D. Abbatt, H. Bozem, P. Hoor, F. Kollner, J. Scchneider, A. Herber, C. Konrad, and R. Brauner, "Effects of 20−100 nm particles on liguid clouds in the clean summertime Arctic," Atmos. Chem. Phys. **16** (17), 11 107−11 124 (2016).

33. *Airborne Measurements for Environmental Research,* Ed. by M. Wendisch and J.-L. Brenguier (Wiley, Weinheim, 2013).

34. A. P. Nagurnyi, "Analysis of data on CO_2 concentration in the surface air layer at the North Pole-35 drifting station (2007−2008)," Meteorol. Gidrol., No. 9, 55−61 (2010).

35. A. P. Nagurnyi and A. P. Makshtas, "Methane concentration in the atmospheric boundary layer from the measurements at North Pole-36 and North Pole-39 drifting ice stations," Russ. Meteorol. Hydrol. **41** (3), 199−204 (2016).

36. I. I. Pipko, S. P. Pugach, and I. P. Semiletov, "CO_2 dynamics on the shelf of the East Siberian Sea," Russ. Meteorol. Hydrol. **35** (9), 624−632 (2010).

37. I. P. Semiletov, N. E. Shakhova, I. I. Pipko, S. P. Pugach, A. N. Charkin, O. V. Dudarev, D. A. Kosmach, and S. Nishino, "Space-time dynamics of carbon and environmental parameters related to carbon dioxide emissions in the Buor-Khaya Bay and adjacent part of Laptev Sea," Biogeosci. **10** (9), 5977−5996 (2013).

38. J. Yu, Z. Xie, L. Sun, H. Kang, P. He, and G. Xing, "$\delta^{13}C$-CH_4 reveals CH_4 variations over oceans from mid-latitudes to the Arctic," Sci. Report **5** (13760), 9 (2015).

39. N. Pankratova, A. Skorokhod, I. Belikov, V. Belousov, V. Muravya, and M. Flint, "Ship-borne observations of atmospheric CH_4 and ^{13}C isotope signature in methane over Arctic seas in summer and autumn 2021," Atmosphere **13** (3), 458 (2022).

40. N. V. Pankratova, I. B. Belikov, V. A. Belousov, V. M. Kopeikin, A. I. Skorokhod, Yu. A. Shtabkin, G. V. Malafeev, and M. V. Flint, "Concentration and isotopic composition of methane, associated gases, and black carbon over Russian Arctic seas (shipborne measurements)," Oceanology **60**, 593−602 (2020).

41. A. I. Skorokhod, N. V. Pankratova, I. B. Belikov, R. L. Thompson, A. N. Novigatsky, and G. S. Golitsyn, "Atmospheric methane and its isotopic composition over seas of the Russian Arctic according to results of ship measurements in summer and autumn of 2015," Dokl. Earth Sci. **470** (5), 580−584 (2016).

42. N. Pankratova, A. Skorokhod, I. Belikov, N. Elansky, V. Rakitin, Y. Shtabkin, and E. Berezina, "Evidence of atmospheric response to methane emissions from the East Siberian Arctic shelf," Geography, Environ., Sustain. **11** (1), 85−92 (2018).

43. A. I. Reshetnikov and A. P. Makshtas, "Arctic Hydrometeorological Observatory "Tiksi"," Trudy GGO, No. 567, 267–283 (2012).

44. P. N. Antokhin, V. G. Arshinova, M. Yu. Arshinov, B. D. Belan, S. B. Belan, D. K. Davydov, G. A. Ivlev, A. V. Kozlov, F. Nedelek, J.-D. Paris, T. M. Rasskazchikova, D. E. Savkin, D. V. Simonenkov, T. K. Sklyadneva, G. N. Tolmachev, and A. V. Fofonov, "Large-scale studies of gaseous and aerosol composition of air over Siberia," Opt. Atmos. Okeana 27 (3), 232–239 (2014).

45. V. G. Arshinova, M. Yu. Arshinov, B. D. Belan, S. B. Belan, D. K. Davydov, G. A. Ivlev, A. V. Kozlov, Ph. Nedelec, J.-D. Paris, T. M. Rasskazchikova, D. E. Savkin, D. V. Simonenkov, T. K. Sklyadneva, G. N. Tolmachev, and A. V. Fofonov, "The vertical distributions of gaseous and aerosol admixtures in air over the Russian Arctic," Atmos. Ocean. Opt. 31 (3), 300–310 (2018).

46. B. D. Belan, G. Ancellet, I. S. Andreeva, P. N. Antokhin, V. G. Arshinova, M. Y. Arshinov, Y. S. Balin, V. E. Barsuk, S. B. Belan, D. G. Chernov, D. K. Davydov, A. V. Fofonov, G. A. Ivlev, S. N. Kotel'nikov, A. S. Kozlov, A. V. Kozlov, K. Law, A. V. Mikhal'chishin, I. A. Moseikin, S. V. Nasonov, P. Nedelec, O. V. Okhlopkova, S. E. Ol'kin, M. V. Panchenko, J.-D. Paris, I. E. Penner, I. V. Ptashnik, T. M. Rasskazchikova, I. K. Reznikova, O. A. Romanovskii, A. S. Safatov, D. E. Savkin, D. V. Simonenkov, T. K. Sklyadneva, G. N. Tolmachev, S. V. Yakovlev, and P. N. Zenkova, "Integrated airborne investigation of the air composition over the Russian sector of the Arctic," Atmos. Meas. Tech. 15 (13), 3941–3967 (2022).

47. V. M. Ivakhov, N. N. Paramonova, V. I. Privalov, I. L. Karol', A. A. Kiselev, A. V. Zinchenko, E. S. Semenets, and V. Yu. Polishchuk, "Observations of methane atmospheric concentration and fluxes at Novy Port station (Yamal peninsula)," Trudy GGO, No. 596, 78–95 (2020).

48. V. A. Poddubny, E. S. Nagovitsyna, Yu. I. Markelov, A. G. Buevich, K. L. Antonov, E. V. Omel'kova, and I. L. Manzhurov, "Estimation of the spatial distribution of methane concentration in the area of the Barents and Kara Seas in summer in 2016–2017," Russ. Meteorol. Hydrol. 45 (3), 193–200 (2020).

49. S. A. Sitnov and I. I. Mokhov, "Anomalies in the atmospheric methane content over Northern Eurasia in the summer of 2016," Dokl. Earth Sci. 480 (1), 637–641 (2018).

50. V. I. Bogoyavlenskii, O. S. Sizov, R. A. Nikonov, I. V. Bogoyavlenskii, and T. N. Kargina, "Earth degassing in the Arctic: The genesis of natural and anthropogenic methane emissions," Arktika: Ekologiya Ekonomika, No. 3, 6–22 (2020).

51. A. Berchet, P. Bousquet, I. Pison, R. Locatelli, F. Chevallier, J.-D. Paris, E. J. Dlugokencky, T. Laurila, J. Hatakka, Y. Viisanen, D. E. J. Worthy, E. Nisbet, R. Fisher, J. France, D. Lowry, V. Ivakhov, and O. Hermansen, "Atmospheric constraints on the methane emissions from the East Siberian Shelf," Atmos. Chem. Phys. 16 (6), 4147–4157 (2016).

52. Y. Li, C. G. Fichot, L. Geng, M. G. Scarratt, H. Xie, "The contribution of methane photoproduction to the oceanic methane paradox," Geophys. Rev. Lett. 47 (14), e2020GL088362 (2020). https://doi.org/10.1029/2020GL088362

53. A. Berchet, I. Pison, P. M. Crill, B. Thornton, Ph. Bousquet, T. Thonat, T. Hocking, J. Thanwerdas, J.-D. Paris, M. Saunois, "Using ship-borne observations of methane isotopic ratio in the Arctic Ocean to understand methane sources in the Arctic," Atmos. Chem. Phys. 20 (6), 3987–3998 (2020).

54. N. Shakhova, I. Semiletov, V. Sergienko, L. Lobkovsky, V. Yusupov, A. Salyuk, A. Salomatin, D. Chernykh, D. Kosmach, G. Panteleev, D. Nicolsky, V. Samarkin, S. Joye, A. Charkin, O. Dudarev, A. Meluzov, and O. Gustafsson, "The East Siberian Arctic shelf: Towards further assessment of permafrost-related methane fluxes and role of sea ice," Philos T. Roy. Soc. A 373, 20140451 (2015). https://doi.org/10.1098/rsta.2014.0451

55. C. J. Sapart, N. Shakhova, I. P. Semiletov, J. Jansen, S. Szidat, D. Kosmach, O. Dudarev, C. van der Veen, M. Egger, V. Sergienko, A. Salyuk, V. Tumskoy, J.-L. Tison, and T. Rockmann, "The origin of methane in the East Siberian Arctic shelf unraveled with triple isotope analysis," Biogeosci. 14 (9), 2283–2292 (2017).

56. N. Shakhova, I. Semiletov, A. Salyuk, V. Yusupov, D. Kosmach, and O. Gustafsson, "Extensive methane venting to the atmosphere from sediments of the East Siberian Arctic shelf," Science 327 (5970), 1246–1250 (2010).

57. K. You, P. B. Flemings, A. Malinverno, T. S. Collett, and K. Darnell, "Mechanisms of methane hydrate formation in geological systems," Rev. Geophys. 57 (4), 1146–1196 (2019).

58. E. G. Nisbet, R. E. Fisher, D. Lowry, J. L. France, G. Allen, S. Bakkaloglu, T. J. Broderick, M. Cain, M. Coleman, J. Fernandez, G. Forster, P. T. Griffiths, C. P. Iverach, B. F. J. Kelly, M. R. Manning, P. B. R. Nisbet-Jones, J. A. Pyle, A. Townsend-Small, A. Shalaan, N. Warwick, and G. Zazzeri, "Methane mitigation: Methods to reduce emissions, on the path to the Paris agreement," Rev. Geophys. 58 (1), e2019RG000675 (2020).

59. V. I. Bogoyavlenskii, A. G. Kazanin, A. V. Kishankov, and G. A. Kazanin, "Dangerous gas-saturated objects in the world ocean: The East Siberian Sea," Arktika: Ekologiya Ekonomika 11 (2), 178–193 (2021).

60. V. I. Bogoyavlenskii, A. V. Kishankov, A. G. Kazanin, and G. A. Kazanin, "Earth degassing in the Arctic: Comprehensive analysis of factors of powerful gas emission in the Laptev Sea," Arktika: Ekologiya Ekonomika 12 (2), 158–171 (2022).

61. K. S. Law and A. Stohl, "Arctic air pollution: Origins and impacts," Science 315 (5818), 1537–1540 (2007).

62. H. Bozem, P. Hoor, D. Kunkel, F. Kollner, J. Schneider, A. Herber, H. Schulz, W. R. Leaitch, A. A. Aliabadi, M. D. Willis, J. Burkart, and J. P. D. Abbatt, "Characterization of transport regimes and the polar dome during Arctic spring and summer using in situ aircraft measurements," Atmos. Chem. Phys. 19 (23), 15049–15071 (2019).

63. A. A. Makosko and A. V. Matesheva, "Assessment of the long-range pollution trends of the atmosphere in the Arctic zone of Russia in 1980–2050 considering cli-

mate change scenarios," Arktika: Ekologiya Ekonomika, No. 1, 45−52 (2020)

64. A. A. Makosko and A. V. Matesheva, "On the assessment of environmental risks from air pollution in the Arctic zone under a changing climate in the XXI century," Arktika: Ekologiya Ekonomika 12 (1), 34−45 (2022).

65. G. V. Alekseev, A. E. Vyazilova, N. I. Glok, N. E. Ivanov, and N. E. Kharalanenkova, "Influence of water temperature anomalies in low ocean latitudes on climate variations in the Arctic and their predictability," Arktika: Ekologiya Ekonomika, No. 3, 73−82 (2019).

66. M. Babin, "Climate change tweaks Arctic marine ecosystems," Science 369 (6500), 137−138 (2020).

67. K. M. Lewis, G. L. van Dijken, and K. R. Arrigo, "Changes in phytoplankton concentration now drive increased Arctic Ocean primary production," Science 369 (6500), 198−202 (2020).

68. M. D. Wendisch, D. Handorf, I. Tegen, R. A. J. Neggers, and G. Spreen, "Glimpsing the ins and outs of the Arctic atmosphere cauldron," EOS, No. 102, EO155959 (2021).

69. M. E. Marushchak, T. Friborg, C. Biasi, M. Herbst, T. Johansson, I. Kiepe, M. Liimatainen, S. E. Lind, P. J. Martikainen, T. Virtanen, H. Soegaard, and N. J. Shurpali, "Methane dynamics in the subarctic tundra: Combining stable isotope analyses, plot- and ecosystem-scale flux measurements," Biogeosci. 13 (2), 597−608 (2016).

70. C. D. Elder, D. R. Thompson, A. K. Thorpe, P. Hanke, A. K. M. Walter,and C. E. Mille, "Airborne mapping reveals emergent power law of Arctic methane emissions," Geophys. Rev. Lett. 47 (3), e2019GL085707 (2020).

71. O. A. Anisimov, S. A. Lavrov, S. A. Zimov, and E. M. Volodin, "Methane emission in the Russian permafrost zone and evaluation of its impact on global climate," Russ. Meteorol. Hydrol. 45 (5), 377−385 (2020).

72. M. Brouillette, "The buried carbon bomb," Nature 591 (7850), 360−362 (2021).

73. M. Jammet, P. Crill, S. Dengel, and T. Friborg, "Large methane emissions from a subarctic lake during spring thaw: Mechanisms and landscape significance," J. Geophys. Res. Biogeosci 120, 2289−2305 (2015).

74. Z. Tan, Q. Zhuang, D. K. Henze, Ch. Frankenberg, E. Dlugokencky, C. Sweeney, A. J. Turner, M. Sasakawa, and T. Machida, "Inverse modeling of pan-Arctic methane emissions at high spatial resolution: What can we learn from assimilating satellite retrievals and using different process-based wetland and lake biogeochemical models?," Atmos. Chem. Phys. 16 (19), 12649−12666 (2016).

75. V. I. Bogoyavlenskii, I. V. Bogoyavlenskii, T. N. Kargina, R. A. Nikonov, and O. S. Sizov, "Earth degassing in the Artic: Remote and field studies of the thermokarst lakes gas eruption," Arktika: Ekologiya Ekonomika, No. 2, 31−46 (2019).

76. L. L. Golubyatnikov and V. S. Kazantsev, "CONTRIBUTION OF TUNDRA LAKES IN WESTERN SIBERIA TO THE ATMOSPHERIC METHANE BUDGET," Izv., Atmos. Ocean. Phys. 49 (4), 395−403 (2013).

77. A. K. M. Walter, S. A. Zimov, G. Grosse, M. C. Jones, P. N. Anthony, F. S. Chapin, J. C. Finlay, M. C. Mack, S. Davydov, P. Frenzel, and S. Frolking, "A shift of thermokarst lakes from carbon sources to sinks during the holocene epoch," Nature 511 (7510), 452−456 (2014).

78. M. Saunois, A. R. Stavert, B. Poulter, Ph. Bousquet, J. G. Canadell, R. B. Jackson, P. A. Raymond, E. J. Dlugokencky, S. Houweling, P. K. Patra, Ph. Ciais, V. K. Arora, D. Bastviken, P. Bergamaschi, D. R. Blake, G. Brailsford, L. Bruhwiler, K. M. Carlson, M. Carrol, S. Castaldi, N. Chandra, C. Crevoisier, P. M. Crill, K. Covey, Ch. L. Curry, G. Etiope, Ch. Frankenberg, N. Gedney, M. I. Hegglin, L. Hoglund-Isaksson, G. Hugelius, M. Ishizawa, A. Ito, G. Janssens-Maenhout, K. M. Jensen, F. Joos, T. Kleinen, P. B. Krummel, R. L. Langenfelds, G. G. Laruelle, L. Liu, T. Machida, Sh. Maksyutov, K. C. McDonald, J. McNorton, P. A. Miller, J. R. Melton, I. Morino, J. Muller, F. Murguia-Flores, V. Naik, Y. Niwa, S. Noce, S. O' Doherty, R. J. Parker, Ch. Peng, Sh. Peng, G. P. Peters, C. Prigent, R. Prinn, M. Ramonet, P. Regnier, W. J. Riley, J. A. Rosentreter, A. Segers, I. J. Simpson, H. Shi, S. J. Smith, L. P. Steele, F. Brett, B. F. Thornton, H. Tian, Y. Tohjima, F. N. Tubiello, A. Tsuruta, N. Viovy, A. Voulgarakis, T. S. Weber, M. van Weele, G. R. van der Werf, R. F. Weiss, D. Worthy, D. Wunch, Y. Yin, Y. Yoshida, W. Zhang, Z. Zhang, Y. Zhao, B. Zheng, Q. Zhu, Q. Zhu, and Q. Qianlai Zhuang, "The global methane budget 2000−2017," Earth Syst. Sci. Data 12 (3), 1561−1623 (2020).

79. M. A. Kuhn, R. K. Varner, D. Bastviken, P. Crill, S. MacIntyre, M. Turetsky, K. W. Anthony, A. D. McGuire, and D. Olefeldt, "BAWLD-CH4: A comprehensive dataset of methane fluxes from boreal and Arctic ecosystems," Earth Syst. Sci. Data 13 (11), 5151−5189 (2021).

80. J. Duncombe, "A climate mystery warns us to heed the unknown," EOS, No. 103 (2022). https://doi.org/10.1029/2022EO220182

81. R. B. Stull, *An Introduction to Boundary Layer Meteorology* (Kluwer Academic Publishers, Norwell, 1988).

82. B. D. Belan, "Dynamics of the atmospheric mixing layer as it follows from data on aerosol," Atmos. Ocean. Opt. 7 (8), 558−562 (1994).

83. S. J. O'Shea, G. Allen, M. W. Gallagher, K. Bower, S. M. Illingworth, J. B. A. Muller, B. T. Jones, C. J. Percival, S. J.-B. Bauguitte, M. Cain, N. Warwick, A. Quiquet, U. Skiba, J. Drewer, K. Dinsmore, E. G. Nisbet, D. Lowry, R. E. Fisher, J. L. France, M. Aurela, A. Lohila, G. Hayman, C. George, D. B. Clark, A. J. Manning, A. D. Friend, and J. Pyle, "Methane and carbon dioxide fluxes and their regional scalability for the European Arctic wetlands during the MAMM project in summer 2012," Atmos. Chem. Phys. 14 (23), 13159−13174 (2014).

84. C. Sweeney, A. Chatterjee, S. Wolter, K. McKain, R. Bogue, S. Conley, T. Newberger, L. Hu, L. Ott, B. Poulter, L. Schiferl, B. Weir, Z. Zhang, and C. E. Miller, "Using atmospheric trace gas vertical profiles to evaluate model fluxes: A case study of Arctic-CAP observations and GEOS simulations for the ABOVE domain," Atmos. Chem. Phys. 22 (9), 6347−6364 (2022).

85. L. Yurganov, F. Muller-Karger, and I. Leifer, "Methane increase over the Barents and Kara Seas after the autumn pycnocline breakdown: satellite observations," Adv. Polar Sci. **30** (4), 382−390 (2019).

86. L. Yurganov, D. Carroll, A. Pnyushkov, I. Polyakov, and H. Zhang, "Ocean stratification and sea-ice cover in Barents and Kara Seas modulate sea−air methane flux: Satellite data," Adv. Polar Sci. **32** (2), 118−140 (2021).

87. A. Panov, A. Prokushkin, K. R. Kubler, M. Korets, A. Urban, M. Bondar, and M. Heimann, "Continuous CO_2 and CH_4 observations in the coastal Arctic atmosphere of the western Taimyr Peninsula, Siberia: The first results from a new measurement station in Dikson," Atmosphere **12** (7), 876 (2021).

88. B. F. Thornton, J. Prytherch, K. Andersson, I. M. Brooks, D. Salisbury, and P. M. Crill, "Shipborne eddy covariance observations of methane fluxes constrain Arctic sea emissions," Sci. Adv. **6** (5), eaay7934 (2020).

89. S. Hartery, R. Commane, J. Lindaas, C. Sweeney, J. Henderson, M. Mountain, N. Steiner, K. McDonald, S. J. Dinardo, C. E. Miller, S. C. Wofsy, and R. Y.-W. Chang, "Estimating regional-scale methane flux and budgets using CARVE aircraft measurements over Alaska," Atmos. Chem. Phys. **18** (1), 185−202 (2018).

90. F. Roth, X. Sun, M. C. Geibel, J. Prytherch, V. Bruchert, S. Bonaglia, E. Broman, F. Francisco Nascimento, A. Norkko, and C. Humborg, "High spatio-temporal variability of methane concentrations challenges estimates of emissions across vegetated coastal ecosystems," Glob Change Biol. **28** (14), 4308−4322 (2022).

91. V. A. Poddubny, E. S. Nagovitsyna, Yu. I. Markelov, A. G. Buevich, K. L. Antonov, E. V. Omel'kova, and I. L. Manzhurov, "Estimation of the spatial distribution of methane concentration in the area of the Barents and Kara Seas in summer in 2016−2017," Russ. Meteorol. Hydrol. **45** (3), 193−200 (2020).

92. Kiselev A.A., Reshetnikov A.I. Metan v Rossiiskoi Arktike: rezul'taty nablyudenii i raschetov // Problemy Arktiki i Antarktidy. 2013. N 2. P. 5−15.

93. O. A. Anisimov, S. A. Lavrov, S. A. Zimov, and E. M. Volodin, "Methane emission in the Russian permafrost zone and evaluation of its impact on global climate," Russ. Meteorol. Hydrol. **45** (5), 377−385 (2020).

94. V. I. Bogoyavlenskii, "Fundamental aspects of the catastrophic gas blowout genesis and the formation of giant craters in the Arctic," Arktika: Ekologiya Ekonomika **11** (1), 51−66 (2021).

95. V. I. Bogoyavlenskii, I. V. Bogoyavlenskii, and T. N. Kargina, "Catastrophic gas blowout in 2020 on the Yamal peninsula in the Arctic. Results of comprehensive analysis of aerospace RS data," Arktika: Ekologiya Ekonomika **1** (3), 362−374 (2021).

96. V. I. Vorob'ev, *Synoptic Meteorology* (Gidrometeoizdat, Leningrad, 1991) [in Russian].

SPELL: OK